Research Article

ENERGY EXPLORATION & EXPLOITATION

Energy Exploration & Exploitation
0(0) 1–14

DOI: 10.1177/0144598719880293
journals.sagepub.com/home/eea
SAGE

Flowing material balance method with adsorbed phase volumes for unconventional gas reservoirs

Guofeng Han[1], **Min Liu**[2] **and Qi Li**[3]

Abstract

This paper presents an improved flowing material balance method for unconventional gas reservoirs. The flowing material balance method is widely used to estimate geological reserves. However, in the case of the unconventional gas reservoirs, such as coalbed methane reservoirs and shale gas reservoirs, the conventional method is inapplicable due to the gas adsorption on the organic pore surface. In this study, a material balance equation considering adsorption phase volume is presented and a new total compressibility is defined. A pseudo-gas reservoir is simulated and the results were compared with the existing formulations. The results show that the proposed formulation can accurately get the geological reserves of adsorbed gas reservoirs. Furthermore, the results also show that the volume of the adsorbed phase has a significant influence on the analysis, and it can only be ignored when the Langmuir volume is negligible.

Keywords

Unconventional gas reservoir, gas initially in place, material balance equation, flowing material balance method, gas adsorption

Introduction

The flowing material balance method uses daily production data to estimate geological reserves by linear regressions. It is one of the most used rate transient analysis methods in oil fields, as it does not require any specialized testing and shut in (Agarwal et al., 1999;

---

[1] Institute of Mechanics, Chinese Academy of Sciences, Beijing, China
[2] Exploration and Development Research Institute of PetroChina Tarim Oilfield Company, Korla, China
[3] Division of Human Resources, North China University of Technology, Beijing, China

Corresponding author:
Guofeng Han, Institute of Mechanics, Chinese Academy of Sciences, Beijing 100190, China.
Email: hanguofeng@imech.ac.cn

Mattar et al., 2006; Mattar and McNeil, 1998; Sun, 2013). Unlike conventional gas reservoirs, the traditionally used flowing material balance method cannot be applied in unconventional gas reservoirs, such as gas shale and coalbed methane, due to the gas adsorption on the organic pore surface (Shen et al., 2018, 2019). Material balance equations (MBEs) are the foundation of flowing material balance methods. King (1993) proposed an MBE for coalbed methane by modifying the deviation factor of gas. Subsequently, other researchers also proposed various forms of MBEs with adsorbed gas, but these equations did not consider the influence of the adsorbed phase volume (Ahmed et al., 2006; Clarkson and Mcgoverm, 2001; Firanda, 2011; Moghadam et al., 2010; Ross and Bustin, 2007). Later, Williams-Kovacs et al. (2012) established an MBE considering adsorbed phase volume. Their studies indicate that the adsorbed phase volume has significant influences on the evaluation results of geological reserves (Zhang et al., 2017).

Based on the MBE considering gas adsorption, some rate transient analysis methods are proposed for gas shale and coalbed methane reservoirs (Clarkson et al., 2007; Clarkson and Salmachi, 2017; Dou et al., 2015; Lewis and Hughes, 2008; Mengal and Wattenbarger, 2011). However, all these methods are based on the King's MBE and do not involve the influence of adsorbed phase volume.

The MBE developed in this study involving adsorbed phase volume is validated from synthetic data. In the first part, a new total compressibility is defined, and the corresponding flowing material balance method considering adsorbed phase volume is proposed. In the second part, case studies have been used to verify the accuracy of this method.

The MBE considering adsorbed phase volume

The following assumptions are made in this paper: (1) the temperature is constant in the gas reservoir production process; (2) the gas dissolved in formation water is neglected; (3) the shrink of matrix by gas desorption is also neglected; (4) gas adsorption satisfies the single component Langmuir equation; (5) the reservoir output does not contain water and is only single-phase gas; (6) the reservoir is up to the saturation of adsorption capacity. The coalbed methane or shale gas is composed of free gas in fractures and adsorption gas in the matrix. The cumulative output of the gas is equal to the difference between the original and remaining reserves of the gas, therefore (Seidle, 2011)

$$G_p = G - \frac{Ah[\phi(1 - S_w) - \phi_a]}{B_g} - Ah\rho_b \frac{V_L p}{p + p_L} \tag{1}$$

$$\phi = \phi_i \exp(-C_f \Delta p) \tag{2}$$

$$S_w = \frac{\phi_i S_{wi} \exp(C_w \Delta p)}{\phi_i \exp(-C_f \Delta p)} = \frac{S_{wi} \exp(C_w \Delta p)}{\exp(-C_f \Delta p)} \tag{3}$$

$$\Delta p = p_i - p \tag{4}$$

where G_p denotes the cumulative production (m^3), G is the gas initially in place (GIIP) (m^3), B_g is the gas volume factor (m^3/m^3), A is the gas reservoir area (m^2), h is the reservoir thickness (m), ϕ is the porosity (%), ϕ_i is the initial porosity (%), ϕ_a is the adsorbed phase apparent porosity (%), S_w is the water saturation (%), S_{wi} is the initial water saturation (%), ρ_b is the rock apparent density (kg/m^3), V_L is the Langmuir volume (m^3/kg), p_L is the Langmuir pressure (MPa), p is the reservoir pressure (MPa), p_i is the initial reservoir pressure (MPa), C_f is the rock pore compressibility (MPa^{-1}), C_w is the formation water compressibility (MPa^{-1}), the subscript i denotes the reservoir initial state.

The adsorbed phase apparent porosity is

$$\phi_a = \frac{V_a}{V} = \frac{Ah\rho_b \frac{\rho_{sc}}{\rho_s}\frac{V_L p}{p_L+p}}{Ah} = \frac{\rho_b \rho_{sc}}{\rho_s}\frac{V_L p}{p_L + p} \tag{5}$$

where V_a is the adsorbed phase volume (m^3), V is the reservoir volume (m^3), ρ_{sc} is the standard state gas density (kg/m^3), ρ_s is the adsorbed phase density (kg/m^3).

Considering the equation of state for real gas, equation (1) can be rewritten as follows

$$\frac{G_p}{G} = 1 - \frac{Ah\phi_i}{G}\frac{Z_{sc}T_{sc}}{p_{sc}T}\frac{p}{Z}\left[\frac{\phi(1-S_w)-\phi_a}{\phi_i} + \frac{\rho_b V_L p_{sc} TZ}{\phi_i Z_{sc} T_{sc}}\frac{1}{p+p_L}\right] \tag{6}$$

where T is the reservoir temperature (K), T_{sc} is the standard state temperature (K), Z is the gas deviation factor at pressure p, Z_{sc} is the gas deviation factor at standard state. The original geological reserves of the gas is

$$\begin{aligned} G &= Ah[\phi_i(1-S_{wi}) - \phi_{ai}]\frac{p_i Z_{sc} T_{sc}}{p_{sc} Z_i T} + Ah\rho_b \frac{V_L p_i}{p_i + p_L} \\ &= Ah\phi_i \frac{Z_{sc}T_{sc}}{p_{sci}T}\frac{p_i}{Z_i}\left[\frac{\phi_i(1-S_{wi})-\phi_{ai}}{\phi_i} + \frac{\rho_b p_{sc} V_L T Z_i}{\phi_i Z_{sc} T_{sc}}\frac{1}{p_i + p_L}\right] \end{aligned} \tag{7}$$

where ϕ_{ai} is the initial adsorbed phase apparent porosity (%).

Defining

$$\frac{p}{Z^*} = \frac{p}{Z}\left[\frac{\phi(1-S_w)-\phi_a}{\phi_i} + \frac{\rho_b V_L p_{sc} TZ}{\phi_i Z_{sc} T_{sc}}\frac{1}{p+p_L}\right] \tag{8}$$

and substituting equations (7) and (8) into equation (6), the following equation is obtained

$$\frac{G_p}{G} = 1 - \frac{p/Z^*}{p_i/Z_i^*} \tag{9}$$

It also can be written as

$$\frac{p}{Z^*} = \frac{p_i}{Z_i^*}\left(1 - \frac{G_p}{G}\right) \tag{10}$$

Equation (10) is the MBE considering adsorbed phase volume for unconventional gas reservoirs, which has the same form as the conventional MBE for gas reservoirs.

Flowing MBE considering adsorbed phase volume

Taking a derivative with respect to time on both sides of equation (10), one gets

$$\frac{d}{dt}\left(\frac{p}{Z^*}\right) = -\frac{p_i q}{Z_i^* G} \tag{11}$$

where q is the production rate (m^3/d). Therefore

$$q = -\frac{Z_i^* G}{p_i}\frac{d}{dt}\left(\frac{p}{Z^*}\right) = -\frac{Z_i^* G}{p_i}\frac{d}{dt}\left\{\frac{p}{Z}\left[\frac{\phi(1-S_w)-\phi_a}{\phi_i} + \frac{\rho_b V_L p_{sc} TZ}{\phi_i Z_{sc} T_{sc}}\frac{1}{p+p_L}\right]\right\} \tag{12}$$

The above equation can be simplified to

$$q = -\frac{Z_i^* G}{p_i}\left[\begin{array}{l}\dfrac{\phi(C_f+S_w C_w)}{\phi_i} + \dfrac{\phi(1-S_w)-\phi_a}{\phi_i}C_g \\ -\dfrac{\rho_b \rho_{sc} V_L}{\phi_i \rho_s}\dfrac{p_L}{(p_L+p)^2} + \dfrac{\rho_b V_L p_{sc} TZ}{\phi_i Z_{sc} T_{sc} p}\dfrac{p_L}{(p+p_L)^2}\end{array}\right]\frac{p}{Z}\frac{dp}{dt} \tag{13}$$

Therefore, equation (13) can be written as

$$q = -\frac{Z_i^* G}{p_i} C_t^* \frac{p}{Z}\frac{dp}{dt} \tag{14}$$

where

$$C_t^* = \frac{\phi(C_f+S_w C_w)}{\phi_i} + \frac{\phi(1-S_w)-\phi_a}{\phi_i}C_g - \frac{\rho_b \rho_{sc} V_L}{\phi_i \rho_s}\frac{p_L}{(p_L+p)^2} + \frac{\rho_b V_L p_{sc} TZ}{\phi_i Z_{sc} T_{sc} p}\frac{p_L}{(p+p_L)^2} \tag{15}$$

With the normalized material balance pseudo-time (Blasingame and Lee, 1988)

$$t_{ca} = \frac{(\mu C_t^*)_i}{q}\int_0^t \frac{q}{\mu C_t^*}\mathrm{d}t = -\frac{(\mu C_t^*)_i Z_i^* G}{q p_i}\int_{p_i}^{p}\frac{p}{\mu Z}\mathrm{d}p = -\frac{C_{ti}^* G^*}{q}\frac{(\mu Z)_i}{p_i}\int_{p_i}^{p}\frac{p}{\mu Z}\mathrm{d}p \tag{16}$$

it can be deduced from equation (8)

$$G^* = \frac{Z_i^* G}{Z_i} = \frac{G}{\frac{\phi_i(1-S_{wi})-\phi_{ai}}{\phi_i} + \frac{\rho_b V_L p_{sc} TZ_i}{\phi_i Z_{sc} T_{sc}}\frac{1}{p_i+p_L}} \tag{17}$$

The flowing material balance method ignoring gas adsorption, i.e. the conventional method, can be obtained when the Langmuir volume (V_L) is zero in equations (5), (8), (15) and (17). If the adsorbed phase apparent porosity $\phi_a = 0$ in equations (8), (15) and (17), it becomes the King's method, which considers gas adsorption but ignores the adsorbed phase volume.

With the normalized pseudo-pressure (Meunier et al., 1987)

$$p_p = \frac{(\mu Z)_i}{p_i} \int_{p_i}^{p} \frac{p}{\mu Z} \mathrm{d}p \tag{18}$$

substituting equation (18) into equation (16), one gets

$$\frac{p_{p_i} - p_p}{q} = \frac{t_{ca}}{C_{ti}^* G^*} \tag{19}$$

The mass conservation equation for unit volume gas is (Kong, 2010)

$$\frac{\partial m}{\partial t} + \nabla \cdot (\rho v) = 0 \tag{20}$$

where v is the seepage velocity (m/d), m is the gas content of unit reservoir volume (kg/m^3)

$$m = \rho[(1 - S_w)\phi - \phi_a] + \frac{\rho_{sc}\rho_b V_L p}{p_L + p} \tag{21}$$

The seepage velocity obeys Darcy's law, as (Kong, 2010)

$$v = -\frac{k}{\mu}\nabla p \tag{22}$$

Therefore, the seepage governing equation is

$$\frac{\partial}{\partial t}\left\{\rho[(1 - S_w)\phi - \phi_a] + \frac{\rho_{sc}\rho_b V_L p}{p_L + p}\right\} = \nabla \cdot \left(\frac{\rho k}{\mu}\nabla p\right) \tag{23}$$

When a well is under constant production rate, according to equations (21) and (10) and provided with the equation of state for real gas, the right side of equation (23) can be written as

$$\frac{\partial}{\partial t}\left\{\rho[(1 - S_w)\phi - \phi_a] + \frac{\rho_{sc}\rho_b V_L p}{p_L + p}\right\} = \frac{\phi_i M}{RT}\frac{p}{Z}C_t^*\frac{\partial p}{\partial t} = \frac{\phi_i M p_i}{Z_i RT}C_{ti}^*\frac{\partial p_p}{\partial t_{ca}} \tag{24}$$

where M is the gas molecular molar mass (kg/mol), R is the universal gas constant, 8.314 J/(mol·K).

The left side of equation (23) is

$$\nabla \cdot \left(\frac{\rho k}{\mu}\nabla p\right) = \nabla \cdot \left(\frac{k}{\mu}\frac{pM}{ZRT}\nabla p\right) = \nabla \cdot \left(\frac{kM}{RT}\frac{p_i}{(\mu Z)_i}\nabla p_p\right) = \frac{kM}{RT}\frac{p_i}{(\mu Z)_i}\nabla^2 p_p \tag{25}$$

The seepage governing equation can be derived by equations (23) to (25) as follows

$$\frac{(\phi\mu C_t^*)_i}{k}\frac{\partial p_p}{\partial t_{ca}} = \nabla^2 p_p \tag{26}$$

This equation has the same form as the governing equation for weakly compressible fluid seepage. Hence, the rate transient analysis can be implemented as the flowing MBE of conventional gas reservoirs.

Method validation

In order to validate the new method presented in this paper, synthetic data of a well production is simulated. The simulation parameters are listed in Table 1. The GIIP calculated by volumetric method is 1.0005×10^8 m^3. Figure 1 shows the simulated production process. In the simulation, B_g, c_g and Z were obtained by the Dranchuk–Purvis–Robinson correlation (Dranchuk et al., 1973), and μ was obtained by the Lee correlation (Lee et al., 1966). The simulation method was explained in Appendix 1.

Table 1. The simulation parameters and GIIPs.

R_e (m)	h (m)	ϕ_i (%)	S_{wi}	p_i (MPa)	T (°C)	*Actual GIIP*
500	5	10	0.2	15	60	1.0005×10^8
M (g/mol)	ρ_b (g/cm^3)	C_f (MPa^{-1})	V_L (m^3/t)	p_L (MPa)	ρ_s (kg/m^3)	*Evaluated GIIP*
16.3	2.65	1.0×10^{-3}	10	6	374	1.0019×10^8

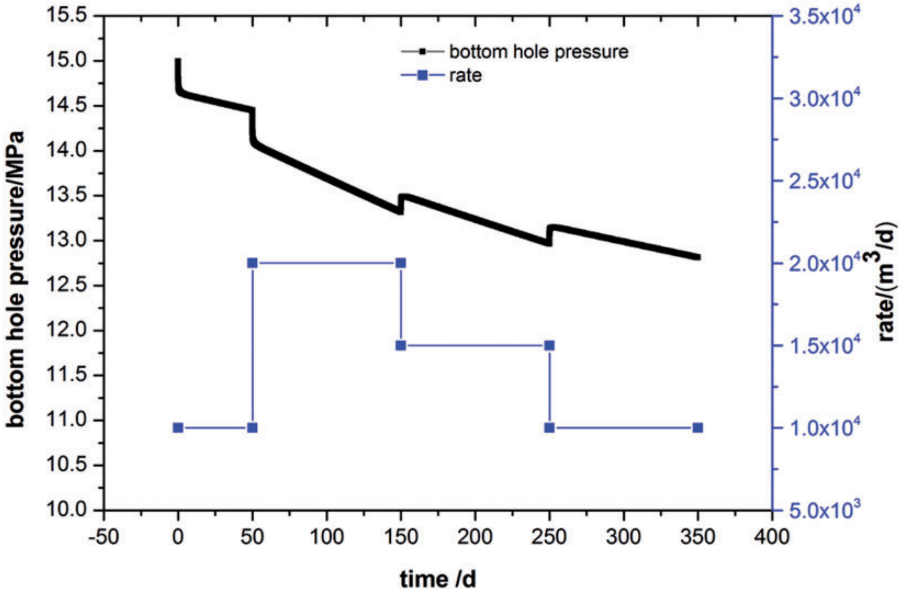

Figure 1. The simulated production – case study.

The results fitted by the flowing material balance method is $G^*=5.6362 \times 10^7$ m^3, shown in Figure 2. According to equation (17), the GIIP determined by the new flowing material balance method is $G = G^* Z_i / Z^* = 5.6362 \times 10^7 \times 0.908892/0.511311 \approx 1.0019 \times 10^8$ m^3. It can be concluded that the GIIP obtained by the new flowing material balance method is much close to the real reserve. Thus, the proposed new method is feasible.

It is more reasonable to use the field data to validate the proposed model. But at that moment we have encountered some difficulties in using the field data to validate the model. On the one hand, the error of many filed data is large, which will affect the verification of the proposed model. On the other hand, when using the field data to verify the proposed model, the GIIP calculated by other methods are required to compare with that obtained by the proposed method. Currently, calculation of GIIP mainly uses the volumetric method, but its accuracy is low. The error caused by these two aspects is likely to be greater than the improvement of the accuracy by the proposed method. Therefore, the conditions for validating the proposed model using field data are not currently available. We will further verify the proposed model with the field data in future research.

Discussion

To test the sensitivity of the developed equation changing one parameter and keeping the other parameters constant in every computation condition, gas well productions are simulated under different reservoir pressures, Langmuir volumes and pressures. The production process used in the simulation is shown in Figure 1. The simulated production data were analyzed by the new method, the conventional method and King's method, and the comparison between the different methods is presented in Figures 3 through 5. The results indicate that errors of the new method are usually below 2%, which is mainly caused by the computation errors.

In the first case, the formation pressure was varied and the corresponding error for different methods was calculated (Figure 3). Error in the estimation of gas reserve for the present formulation is around 2%. It is clear from Figure 3 that ignoring gas adsorption can

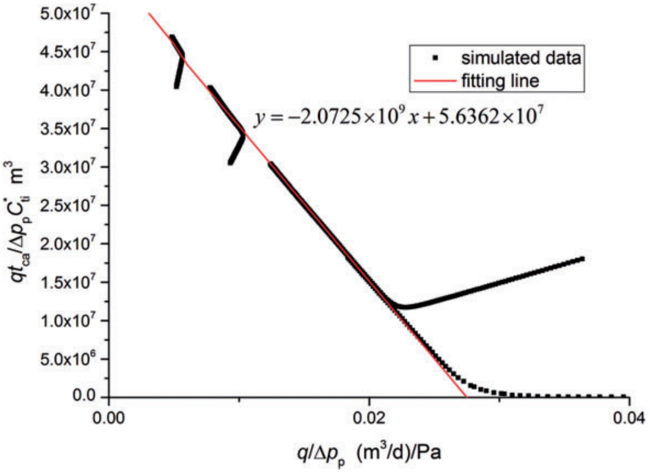

Figure 2. The fitting by the new flowing material balance method.

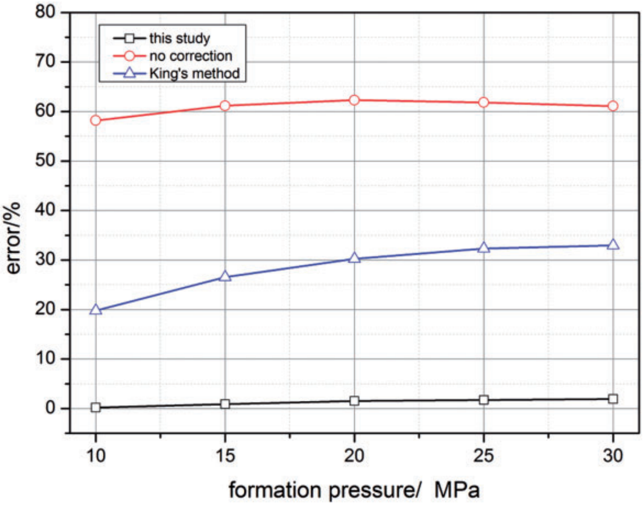

Figure 3. The influence of reservoir pressures on the error.

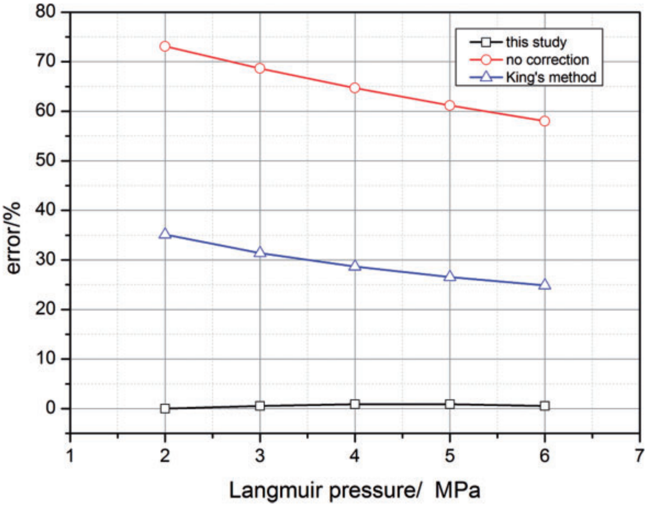

Figure 4. The influence of Langmuir pressures on the error.

cause an error of approximately 60%. The errors increase marginally with the increase of reservoir pressure, and then decrease a bit. The errors of King's method increase with the increase of reservoir pressure, and the increasing rate tends to be slow as the formation pressure increases. With an increase of the formation pressure from 10 MPa to 30 MPa, the errors increase from about 20% to 33%.

In the second case, the Langmuir pressure was varied and the corresponding error for different methods was calculated (Figure 4). Error in the estimation of gas reserve for the present formulation is around 2%. It is clear from Figure 4 that the errors in the conventional method and King's method decrease with the increase of Langmuir pressure, and the

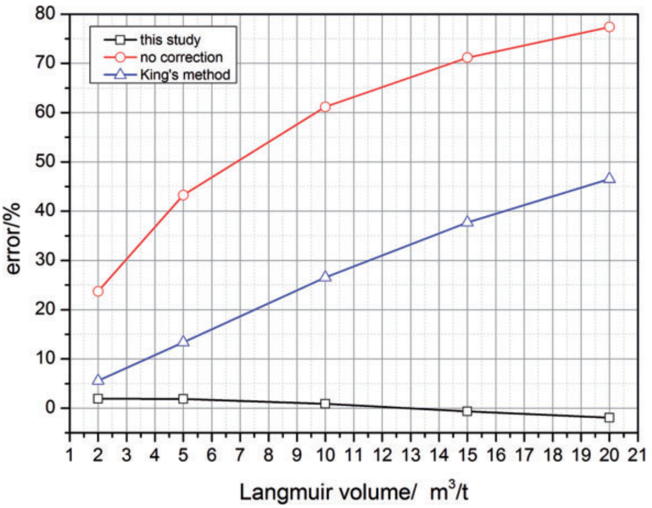

Figure 5. The influence of Langmuir volumes on the error.

decreasing rate tends to be slow. When the Langmuir pressure increases from 2 MPa to 6 MPa, the errors of ignoring gas adsorption decrease from 73% to 58%, and that of King's method decrease from 35% to 25%.

In the third case, the Langmuir volume was varied and the corresponding error for different methods was calculated (Figure 5). Error in the estimation of gas reserve for the present formulation is around 2%. It is clear from Figure 5 that the errors of ignoring gas adsorption increase with the increase of Langmuir volumes. When the Langmuir volume increases from 2 m^3/t to 20 m^3/t, the errors of ignoring gas adsorption increase from 24% to 77%. And when King's method is used, the errors increase from 6% to 47%. Ignoring the gas adsorption could cause very large errors, even wrong results. Therefore, the adsorbed phase volume can cause distinct influences. Only when the Langmuir volume is very small, it can be neglected.

The adsorbed phase methane densities obtained by researchers have some differences. The results by Dubinin (1960), Haydel and Kobayashi (1967), Ambrose et al. (2012), Mavor et al. (2004) are 0.371, 0.374, 0.34, 0.4223 g/cm^3, respectively. In the fourth case, the adsorbed phase densities were varied and the corresponding error for different methods was calculated (Figure 6). Errors in the estimation of gas reserve for the present formulation are around 2%. It can be found that the errors of the King's method and ignoring gas adsorption decrease with the adsorbed phase density. The errors of ignoring gas adsorption are above 50%. The errors of King's method are not less than 20%, based on those researcher's data. The errors of the new method are below 2%.

The theory of the FMB method shows that when the flow of the reservoirs is in the pseudo-steady state, the plots of $q/\Delta p_p – qt_{ca}/\Delta p_p c^*_{ti}$ of different production rates are on the same line. Figure 2 proves this. When adopting King's method or the conventional no correction method, it only needs to replace c^*_{ti} with the corresponding total compressibility. It is easy to find that these do not change the nature of plots of $q/\Delta p_p – qt_{ca}/\Delta p_p c^*_{ti}$ for different production rates on the same straight line. Therefore, it can be concluded that the analysis error is independent of the production rate. In order to solve the effects of

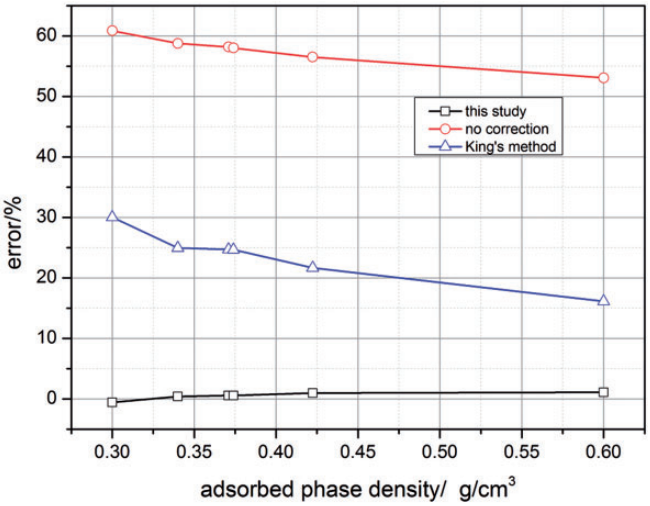

Figure 6. The influence of adsorbed phase densities on the error.

the unsteady production rate, Blasingame proposed the concept of material balance pseudo-time to replace real physical time. (It can be obtained by replacing c_{ti}^{*} in equation (16) with a total compressibility.) This can greatly reduce the impact of changes in production rates. Especially, when the reservoir flow is close to the pseudo-steady state, the gradual change in production rate has almost no effect on the plots of $q/\Delta p_p–qt_{ca}/\Delta p_p c_{ti}^{*}$.

Hypotheses (1), (2) and (6) are suitable for various gas reservoirs. Therefore, their influence can be ignored. If the gas well produces water, the downhole pressure will decrease faster than that of the hypothetical case that no water is produced with the same gas production rate. The GIIP assessed by the proposed method would be smaller than the actual one. The rock shrinkage due to gas desorption increases the pore volume, thereby reducing the reservoir pressure. In the same production situation, the downhole pressure will decrease faster than that of the hypothetical case that the gas desorption is not considered. Therefore, the GIIP will be underestimated by the proposed method.

Conclusion

An improved flowing material balance for unconventional gas reservoirs was presented in this study to estimate their storage. Based on the unconventional gas reservoir MBE considering adsorbed phase volume, (1) a new total compressibility is defined and (2) a flowing material method considering adsorbed phase volume for unconventional gas reservoirs is proposed. Major conclusions based on the case study are as follows:

- The cases study indicated that the new flowing material balance method developed in the present study can determine the GIIP correctly.
- Analysis results under different reservoir pressures, Langmuir volumes and pressures demonstrate that ignoring gas adsorption can make large errors.
- The adsorbed phase volume has a significant influence on the results, and only when the Langmuir volume is small and reservoir pressure is large, it can be neglected.

Declaration of conflicting interests

The author(s) declared no potential conflicts of interest with respect to the research, authorship, and/or publication of this article.

Funding

The author(s) disclosed receipt of the following financial support for the research, authorship, and/or publication of this article: This work was supported by the National Natural Science Foundation of China (No. 11602276).

ORCID iD

Guofeng Han https://orcid.org/0000-0002-6536-7378

References

Agarwal RG, Gardner DC and Kleinsteiber SW (1999) Analyzing well production data using combined type curve and decline curve concepts. *SPE Reservoir Evaluation & Engineering* 2(5): 478–486.

Ahmed TH, Centilmen A and Roux BP (2006) A generalized material balance equation for coalbed methane reservoirs. In: *Proceedings of the SPE annual technical conference and exhibition*, San Antonio, Texas, USA, 24–27 September 2006.

Ambrose RJ, Hartman RC, Diaz-Campos M, et al. (2012) Shale gas-in-place calculations: Part I – New pore-scale considerations. *SPE Journal* 17(1): 219–229.

Blasingame TA and Lee WJ (1988) The variable-rate reservoir limits testing of gas wells. In: *SPE Gas Technology Symposium*, Dallas, Texas, 13–15 June 1988.

Clarkson CR, Bustion RM and Seidle JP (2007) Production-data analysis of single-phase (gas) coalbed-methane wells. *SPE Reservoir Evaluation & Engineering* 10(3): 312–331.

Clarkson CR and Mcgoverm JM (2001) Study of the potential impact of matrix free gas storage upon coalbed gas reserves and production using a new material balance equation. In: *Proceedings of the 2001 international coalbed methane symposium*, Tuscaloosa, Alabama, USA, 14–18 May 2001.

Clarkson CR and Salmachi A (2017) Rate-transient analysis of an undersaturated CBM reservoir in Australia: Accounting for effective permeability changes above and below desorption pressure. *Journal of Natural Gas Science and Engineering* 40: 51–60.

Dou X, Liao X, Zhao X, et al. (2015) Quantification of permeability stress-sensitivity in tight gas reservoir based on straight-line analysis. *Journal of Natural Gas Science and Engineering* 22: 598–608.

Dranchuk PM, Purvis RA and Robinson DB (1973) Computer calculations of natural gas compressibility factors using the standing and Katz correlation. In: *Petroleum Society of Canada annual technical meeting*, Edmonton, 8–12 May 1973.

Dubinin MM (1960) The potential theory of adsorption of gases and vapors for adsorbents with energetically nonuniform surfaces. *Chemical Reviews* 60(2): 235–241.

Firanda E (2011) The development of material balance equations for coalbed methane reservoirs. In: *Proceedings of the SPE Asia Pacific oil and gas conference and exhibition*, Jakarta, Indonesia, 20–22 September 2011.

Haydel JJ and Kobayashi R (1967) Adsorption equilibria in the methane-propane-silica gel system at high pressures. *Industrial & Engineering Chemistry Fundamentals* 6(4): 564–554.

King GR (1993) Material balance techniques for coal seam and Devonian shale gas reservoirs with limited water influx. *SPE Reservoir Engineering* 8(1): 67–72.

Kong XY (2010) *Advanced Transport in Porous Media*. 2nd ed. Heifei: Press of University of Science and Technology of China.

Lee AL, Gonzalez MH and Eakin BE (1966) The viscosity of natural gases. *Journal of Petroleum Technology* 18(8): 997–1000.

Lewis AM and Hughes RG (2008) Production data analysis of shale gas reservoirs. In: *Proceedings of the SPE annual technical conference and exhibition*, Denver, Colorado, USA, 21–24 September 2008.

Mattar L, Anderson D and Stotts G (2006) Dynamic material balance oil or gas-in-place without shut-Ins. *Journal of Canadian Petroleum Technology* 45(11): 7–10.

Mattar L and McNeil R (1998) The flowing gas material balance. *Journal of Canadian Petroleum Technology* 37(2): 52–55.

Mavor MJ, Hartman C and Pratt TJ (2004) Uncertainty in sorption isotherm measurements. In: *Proceedings of the international coalbed methane symposium*, Tuscaloosa, Alabama, 14–16 May 2004.

Mengal SA and Wattenbarger RA (2011) Accounting for adsorbed gas in shale reservoirs. In: *Proceedings of the SPE middle east oil and gas show and conference*, Manama, Bahrain, 25–28 September 2011.

Meunier DF, Kabir CS and Wittmann MJ (1987) Gas well test analysis: Use of normalized pseudo-variables. *SPE Formation Evaluation* 2(4): 629–636.

Moghadam S, Jeje O and Mattar L (2010) Advanced gas material balance in simplified format. *Journal of Canadian Petroleum Technology* 50(1): 90–98.

Ross DJK and Bustin M (2007) Impact of mass balance calculations on adsorption capacities in microporous shale gas reservoirs. *Fuel* 86: 2696–2706.

Seidle J (2011) *Fundamentals of Coalbed Methane Reservoir Engineering*. Tulsa: PennWell Corporation.

Shen WJ, Song FQ, Hu X, et al. (2019) Experimental study on flow characteristics of gas transport in micro- and nanoscale pores. *Scientific Reports* 9: 10196.

Shen WJ, Zheng LG, Oldenberg CM, et al. (2018) Methane adsorption and diffusion in shale rocks – A numerical study using the dusty gas model in Tough2/EOS7C-ECBM. *Transport in Porous Media* 123(3): 521–531.

Sun H (2013) *Advanced Production Decline Analysis and Application*. Beijing: Petroleum Industry Press, pp.134–137.

Williams-Kovacs J, Clarkson CR and Nobakht M (2012) Impact of material balance equation selection on rate-transient analysis of shale gas. In: *Proceedings of the SPE annual technical conference and exhibition*, San Antonio, Texas, USA, 8–10 October 2012.

Zhang X, Wang X, Hou X, et al. (2017) Rate decline analysis of vertically fractured wells in shale gas reservoirs. *Energies* 10: 1602.

Appendix 1. Simulation method

Consider an unconventional gas reservoir with circular boundary and the production well is located at the center of the circle. The governing equation for gas well production is given by equation (23). When gas wells are produced, the inner and outer boundary conditions are as follows, respectively

$$2\pi r_w h \frac{K}{\mu}\frac{\partial p}{\partial r}|_{r=r_w} = B_g q \tag{27}$$

$$\frac{\partial p}{\partial r}|_{r=r_e} = 0 \tag{28}$$

where r_e is the reservoir radius (m). At the beginning, the reservoir is full of original reservoir pressure, so the initial conditions can be written as

$$p(r, 0) = p_i \tag{29}$$

The radial coordinate of the above equations are transformed as follows

$$r = r_w e^x \tag{30}$$

For the convenience of writing, the following variables are defined

$$A = \phi_i \frac{p}{Z} C_t^* r_w^2 e^{2x}, \quad B = \frac{pk}{\mu Z}, \quad E = 2\pi h \frac{k}{\mu e^x} \tag{31}$$

Thus, the above governing equation (23), boundary conditions (27) and (28) and initial condition (29) can be written as follows

$$A \frac{\partial p}{\partial t} = \frac{\partial}{\partial x}\left(B \frac{\partial p}{\partial x} \right) \tag{32}$$

$$p(x, 0) = p_i \tag{33}$$

$$E \frac{\partial p}{\partial x}|_{x=0} = B_g q \tag{34}$$

$$\frac{\partial p}{\partial x}|_{x=x_e} = 0 \tag{35}$$

The distance from the wellbore to the outer boundary is discretized into N segments, numbering the nodes from 0 to N. The spatial step is Δx and the time step is Δt. The difference equations of the governing equation (32) and the boundary conditions (34) and (35) are as follows, respectively

$$A_j^s \frac{p_j^{(s+1)} - p_j^n}{\Delta t} = \frac{1}{\Delta x}\left[B_{j+\frac{1}{2}}^{(s)} \frac{p_{j+1}^{(s+1)} - p_j^{(s+1)}}{\Delta x} - B_{j-\frac{1}{2}}^{(s)} \frac{p_j^{(s+1)} - p_{j-1}^{(s+1)}}{\Delta x} \right] \tag{36}$$

$$E_0^{(s)} \frac{p_1^{(s+1)} - p_{-1}^{(s+1)}}{2\Delta x} = B_g q^{(s)} \tag{37}$$

$$\frac{p_{N+1}^{(s+1)} - p_{N-1}^{(s+1)}}{2\Delta x} = 0 \tag{38}$$

where subscript j indicates the node number; superscript n indicates the nth time step; superscript s in the parentheses indicates the sth iteration of a time step. In order to construct a boundary condition difference scheme of second-order precision, two virtual nodes numbered –1 and $N + 1$ are added. Defining

$$\theta = \frac{\Delta t}{\Delta x^2}, \quad \tau = \frac{\Delta t}{\Delta x} \tag{39}$$

Therefore, the above equations (36) to (38) can be simplified to

$$A_j^s p_j^n = -\theta B_{j+\frac{1}{2}}^{(s)} p_{j+1}^{(s+1)} + \left(\theta B_{j+\frac{1}{2}}^{(s)} + \theta B_{j-\frac{1}{2}}^{(s)} + A_j^s\right) p_j^{(s+1)} - \theta B_{j-\frac{1}{2}}^{(s)} p_{j-1}^{(s+1)} \tag{40}$$

$$E_0^{(s)} p_1^{(s+1)} - E_0^{(s)} p_{-1}^{(s+1)} = 2\Delta x B_g q^{(s)} \tag{41}$$

$$p_{N+1}^{(s+1)} - p_{N-1}^{(s+1)} = 0 \tag{42}$$

By combining the initial conditions and the production rate with the above equations, a linear equation set of $N+3$ orders can be formed, so that the pressure of the $N+1$ nodes and the other two virtual nodes can be solved.